Journal of the Korea Concrete Institute
Vol.17 No.4, pp.637~643, August, 2005

Anchor Design to Prevent Debonding of Repair Mortar in Repaired Concrete Members

Dong-Uk Choi[1)]*and Chin-Yong Lee[2)]

[1)]*Dept. of Architectural Engineering, Hankyong National University, Ansung 456-240, Korea*
[2)]*CareCon, Co, Ltd., Seoul 134-030, Korea*

(Received July 20, 2004, Accepted May 30, 2005)

Abstract

Reinforced concrete beams or slabs are often strengthened or repaired using polymer modified cement concrete. Stresses can develop in the structure by ambient temperature changes because thermal coefficients of the repair material and the existing concrete are typically different. Especially, shear stress often causes debonding of the interface. In this study, a rational procedure was developed where anchors can be designed in strengthened or repaired concrete members to prevent debonding at the interface. The current design procedure considers thicknesses and elastic moduli of the repair material and existing concrete, ambient temperature change, length, and beam-vs.-slab action. The procedure is also applicable to stresses developed by differential drying shrinkage.

Keywords: anchors, interface delamination, shear stress, temperature change, differential shrinkage

1. Introduction

The reinforced concrete beams or slabs are often strengthened or repaired using polymer modified cement concrete. In the repaired beams or slabs at early ages, internal stresses can develop due to drying shrinkage of the repair material. Because the thermal coefficients of the repair material and the existing concrete are typically different, stresses also develop as the structure is subjected to ambient temperature changes. These environmentally-induced stresses can sometimes be large enough to cause damage to the structure, such as tensile cracks in the repair material, debonding of the interface between the two materials, and horizontal cracking in the existing concrete.[1)] Especially, debonding of the interface or interface delamination is often observed in the field. When it is desired to use anchors to prevent interface delamination in the repaired structures, there is a lack of design guidelines.

In this study, an existing closed-form solution was first used to determine distribution of the thermally-induced interface shear stress in a repaired beam. The results of parametric study that investigated variables influencing the stress development in repaired concrete beams or slabs are introduced. Then an anchor design procedure to prevent interface delamination of the repaired concrete members is developed. Effect of both temperature change and differential drying shrinkage is included.

* *Corresponding author*
E-mail address: choidu@hknu.ac.kr

2. Shear stress distribution at interface

An analytical procedure proposed by Chen et al.[2)] provides exact solutions of the thermally-induced stresses of a composite beam as far as the linear elastic material properties, i.e. elastic modulus (E), Poisson's Ratio (v), and coefficient of thermal expansion (α), of the two layers of the repaired beam of Fig. 1 remain the same and the beam is subjected to a uniform temperature change.

Using the material properties shown in Table 1, the thermally-induced shear stress (tau-xy, τ_{xy}) developed by temperature drop of 20 degree Celsius (ΔT = -20 °C), for example, along the interface of the repaired beam is shown in Fig. 2(a). The interface shear stress develops only close to the beam end as shown in Fig. 2(a). The high τ_{xy} that develops toward the beam end is the cause of the interface delamination. It is noted in Fig. 2(b) that the distance τ_{xy} develops is approximately the same as the total depth ($H_{total} = H_1 + H_2$) of the repaired beam. Fig. 2(c) shows τ_{xy} distribution across

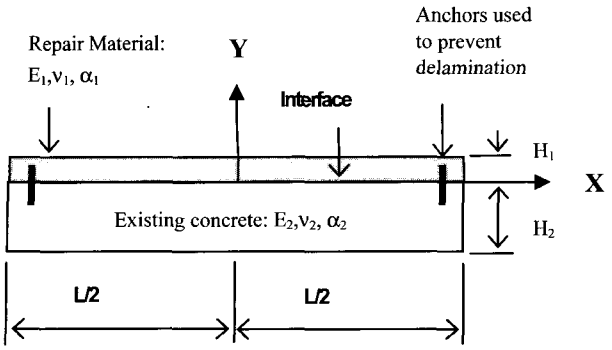

Fig. 1 A composite beam: $\alpha_1 > \alpha_2$

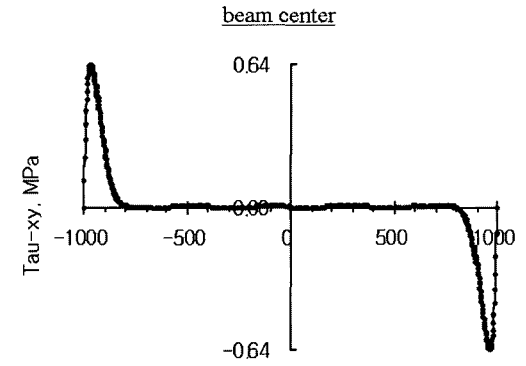

(a) τ_{xy} distribution at interface

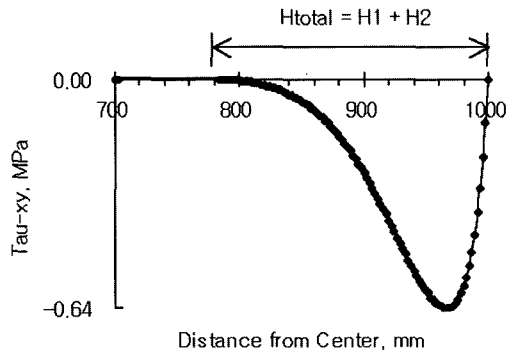

(b) τ_{xy} distribution toward beam end

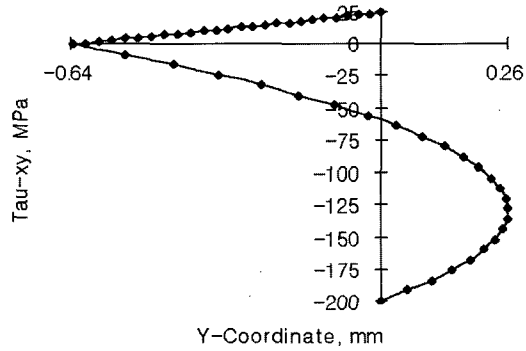

(b) τ_{xy} distribution across beam cross-section

Fig. 2 τ_{xy} Distribution at interface in repaired beam of Fig. 1 and Table 1[2)]

beam cross-section which reveals that the maximum τ_{xy} develops at the interface.

3. Variables affecting stress development

3.1 Ratio of thicknesses and elastic moduli

In previous studies by Hess[3)] and Choi et al.,[4)] the major variables influencing the stress development in a composite beam subjected to temperature changes were suggested as the following:

- Thickness ratio of the two layers, $m = H_1 / H_2$
- Modular ratio of the two layers, $n = E_1 / E_2$

Analyses using Chen et al.'s method were performed using the range of material properties often encountered in the field as summarized in Table 2 to determine maximum interface shear stresses induced in repaired beams by temperature changes: i.e. max. τ_{xy} at the interface. Length and width of the beam assumed were 2,000 mm and 1.0 mm (unit width), respectively.

The analysis results summarized in Figs. 3 through 5 reveal that the max. τ_{xy} at the interface increases as the thickness of the repair material (H_1) increases [or the thickness ratio (m) increases]. The max. τ_{xy} at the interface also increases as the elastic modulus of the repair material (E_1) increases [or the modular ratio (n) increases].

Table 1 Material properties

Layer	E, MPa	H, mm	α, m/m/°C	ν	ΔT, °C	Remarks
1	15,000	25	20×10^{-6}	0.20	-20	repair material
2	25,000	200	10×10^{-6}	0.18		existing concrete

Note: beam length = 2,000 mm, width = unit width

Table 2(a) Thicknesses included in analyses, unit = mm

H_1	5	10	15	20	30	40	50	60	70	80	90
H_2	200										

Table 2(b) Elastic moduli included in analyses, unit = MPa

E_1	2,500	5,000	10,000	15,000	20,000	25,000	30,000
E_2	20,000; 25,000; 30,000						

Table 2(c) Thermal coefficients and temperature change

Layer	α, m/m/°C	ΔT, °C	Remarks
1	20×10^{-6}	-20	repair material
2	10×10^{-6}		existing concrete

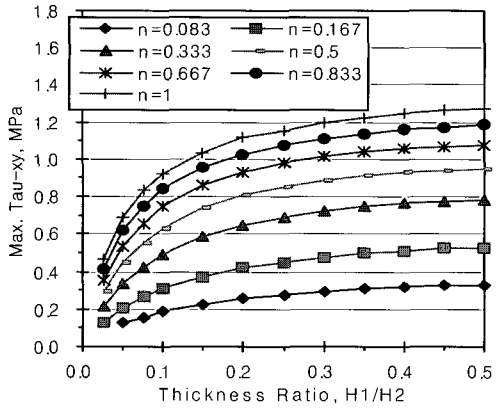

Fig. 3 Max. τ_{xy} at interface vs. thickness ratio (m):
E_2 = 20,000 MPa, H_2 = 200 mm, $\Delta\alpha\Delta T$ = -200*10^{-6} m/m,
E_1 = 2,500 MPa (n = 0.125) ~ 30,000 MPa (n = 1.5)

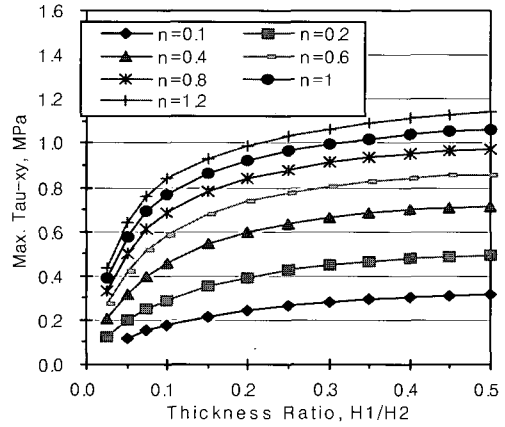

Fig. 4 Max. τ_{xy} at interface vs. thickness tatio (m):
E_2 = 25,000 MPa, H_2 = 200 mm, $\Delta\alpha\Delta T$ = -200*10^{-6} m/m,
E_1 = 2,500 MPa (n = 0.1) ~ 30,000 MPa (n = 1.2).

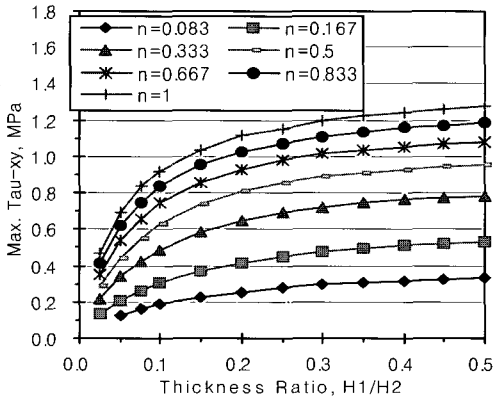

Fig. 5 Max. τ_{xy} at interface vs. thickness ratio (m):
E_2 = 30,000 MPa, H_2 = 200 mm, $\Delta\alpha\Delta T$ = -200*10^{-6} m/m,
E_1 = 2,500 MPa (n = 0.083) ~ 30,000 MPa (n = 1.0)

3.2 Effective strain: $\Delta\alpha\Delta T$

In this study the effective strain is defined as the difference of the thermal coefficients between the repair material and existing concrete multiplied by temperature change, i.e. $\Delta\alpha\Delta T = (\alpha_1 - \alpha_2) * \Delta T$. It is noted that, in Table 2 and Figs. 3 through 5, the difference in the thermal coefficients, $\Delta\alpha$, is 10 * 10^{-6} m/m/°C while the temperature drop is 20 °C resulting in $\Delta\alpha\Delta T$ = -200 * 10^{-6} m/m. When the actual $\Delta\alpha\Delta T$ is different from -200 * 10^{-6} m/m, the max. τ_{xy} developed should be linearly proportioned using a factor of (actual $\Delta\alpha\Delta T$) / (-200 * 10^{-6}).

3.3 Elastic modulus of existing concrete

In Fig. 3, the elastic modulus of existing concrete (E_2) is 20,000 MPa representing a low strength concrete (f_{ck} = 18.1 MPa). In Figs. 4 and 5, E_2 is 25,000 MPa (f_{ck} = 28.2 MPa) and 30,000 MPa (f_{ck} = 40.7 MPa), respectively, each representing medium and high strength existing concretes. Figs. 3 through 5 reveal that the max. τ_{xy} at the interface increase as E_2 increases from 20,000 MPa to 25,000 MPa and 30,000 MPa, respectively, when the thickness and modular ratios remain the same. Tables 3 through 5 summarize the max. τ_{xy} developed at the interface for low, medium, and high strength existing concrete, respectively.

3.4 Thickness of existing concrete

In Tables 3 through 5 (and also in Figs. 3 through 5), the thickness of the existing concrete is 200 mm. The thicknesses of 300 mm and 400 mm were also analyzed. The analysis results reveal that the max. τ_{xy} at the interface remain the same for the same thickness and modular ratios.

3.5 Length

In Tables 3 through 5 (and also in Figs. 3 through 5), the beam length is 2.0 m. Results of analyses using longer and shorter beam lengths of 4.0 m, 1.0 m, and 0.5 m reveal that the max. τ_{xy} at the interface does not change when the thickness and modular ratios remain the same.

3.6 Beam vs. slab action

Fowler et al.[5] suggested that a beam stress (plane stress) can be approximately converted to a slab stress (plane strain) by using a 1 / (1 - ν) factor where the Poisson's Ratio (ν) is that of the repair material. Comparing the current analysis results in plane stress with the existing analysis results in plane strain of reference 4, the suggested factor resulted in stresses close to more elaborate analytical results.

3.7 Effect of creep

While the thermally-induced stresses develop from a mismatch in the coefficients of thermal expansion between the two different materials (repair material and existing concrete), stresses can also develop, especially at early ages,

Table 3 Summary of max. τ_{xy} at interface: low strength existing concrete, unit = MPa

E_2 = 20,000 MPa, H_2 = 200 mm, ν_1 = 0.20, ν_2 = 0.18, $\Delta\alpha\Delta T$ = -200 * 10^{-6} m/m

E_1, MPa		2,500	5,000	10,000	15,000	20,000	25,000	30,000
n		0.125	0.25	0.5	0.75	1	1.25	1.5
H_1, mm	m							
5	0.025	0.0713	0.1186	0.1939	0.2564	0.3111	0.3598	0.4038
10	0.050	0.1123	0.1847	0.2968	0.3856	0.4597	0.5236	0.5791
15	0.075	0.1428	0.2331	0.3683	0.4708	0.5530	0.6214	0.6795
20	0.10	0.1666	0.2705	0.4206	0.5298	0.6150	0.6836	0.7407
30	0.15	0.2024	0.3250	0.4921	0.6060	0.6907	0.7570	0.8109
40	0.20	0.2281	0.3627	0.5382	0.6530	0.7370	0.8028	0.8568
50	0.25	0.2418	0.3899	0.5701	0.6859	0.7706	0.8375	0.8930
60	0.30	0.2620	0.4097	0.5927	0.7096	0.7959	0.8649	0.9227
70	0.35	0.2734	0.4244	0.6087	0.7270	0.8154	0.8870	0.9478
80	0.40	0.2818	0.4350	0.6202	0.7399	0.8305	0.9051	0.9691
90	0.45	0.2884	0.4423	0.6282	0.7496	0.8425	0.9197	0.9870
100	0.50	0.2929	0.4471	0.6332	0.7564	0.8521	0.9323	1.0022

Table 4 Summary of max. τ_{xy} at interface: medium strength existing concrete, unit = MPa

E_2 = 25,000 MPa, H_2 = 200 mm, ν_1 = 0.20, ν_2 = 0.18, $\Delta\alpha\Delta T$ = -200 * 10^{-6} m/m

E_1, MPa		2,500	5,000	10,000	15,000	20,000	25,000	30,000
n		0.1	0.2	0.4	0.6	0.8	1	1.2
H_1, mm	m							
5	0.025		0.1259	0.2074	0.2754	0.3350	0.3889	0.4380
10	0.050	0.1190	0.1972	0.3197	0.4184	0.5020	0.5746	0.6395
15	0.075	0.1515	0.2497	0.3993	0.5153	0.6107	0.6913	0.7609
20	0.10	0.1771	0.2906	0.4589	0.5852	0.6857	0.7687	0.8386
30	0.15	0.2153	0.3508	0.5421	0.6777	0.7810	0.8633	0.9310
40	0.20	0.2426	0.3931	0.5975	0.7364	0.8397	0.9213	0.9884
50	0.25	0.2635	0.4240	0.6362	0.7769	0.8809	0.9633	1.0315
60	0.30	0.2796	0.4472	0.6638	0.8057	0.9109	0.9949	1.0652
70	0.35	0.2920	0.4643	0.6834	0.8263	0.9331	1.0193	1.0921
80	0.40	0.3017	0.4769	0.6971	0.8413	0.9496	1.0381	1.1139
90	0.45	0.3089	0.4860	0.7068	0.8519	0.9623	1.0531	1.1314
100	0.50	0.3142	0.4920	0.7128	0.8589	0.9715	1.0652	1.1465

Table 5 Summary of max. τ_{xy} at interface: high strength existing concrete, unit = MPa

E_2 = 30,000 MPa, H_2 = 200 mm, ν_1 = 0.20, ν_2 = 0.18, $\Delta\alpha\Delta T$ = -200 * 10^{-6} m/m

E_1, MPa		2,500	5,000	10,000	15,000	20,000	25,000	30,000
n		0.083	0.167	0.333	0.5	0.667	0.833	1
H_1, mm	m							
5	0.025		0.1325	0.2183	0.2909	0.3553	0.4133	0.4667
10	0.050	0.1250	0.2075	0.3386	0.4452	0.5370	0.6178	0.6895
15	0.075	0.1589	0.2632	0.4247	0.5524	0.6586	0.7501	0.8358
20	0.10	0.1855	0.3070	0.4905	0.6309	0.7452	0.8408	0.9225
30	0.15	0.2255	0.3719	0.5840	0.7382	0.8578	0.9552	1.0360
40	0.20	0.2545	0.4178	0.6467	0.8073	0.9286	1.0255	1.1166
50	0.25	0.2763	0.4518	0.6913	0.8551	0.9776	1.0750	1.1559
60	0.30	0.2934	0.4772	0.7236	0.8890	1.0126	1.1113	1.1939
70	0.35	0.3069	0.4968	0.7467	0.9131	1.0378	1.1384	1.2231
80	0.40	0.3170	0.5111	0.7629	0.9304	1.0565	1.1585	1.2457
90	0.45	0.3251	0.5214	0.7741	0.9423	1.0699	1.1743	1.2637
100	0.50	0.3309	0.5288	0.7814	0.9499	1.0790	1.1858	1.2782

due to a differential drying shrinkage (i.e. drying shrinkage difference between the newly cast repair material and the existing concrete). In principle, the shrinkage-induced stresses can be analyzed in a similar way to the thermal stress analysis as the amount of the differential shrinkage can replace the effective strain previously defined in section 3.2 (mismatch of thermal coefficients of the two materials multiplied by the temperature change).

$$\Delta\varepsilon_{sh} = \varepsilon_{sh,1} - \varepsilon_{sh,2} = \Delta\alpha\Delta T \quad (1)$$

It is noted, however, that most drying shrinkage develops at early ages and creep effect (or stress relaxation) may play an important role. In a study, where the experimentally measured shrinkage-induced interface stresses at early ages was compared to the theoretical solutions determined using the analytical method proposed by Chen et al., the significant differences between the theoretically- and experimentally-determined shear stresses were observed (theoretical τ_{xy} < experimental τ_{xy}).[6] Using a research result of Silfwerbrand who proposed an analytical procedure for the shrinkage-induced stress problems where a creep constant was used to include the creep effect, E_1 of the current analysis can be converted to reduced elastic modulus E_r to include the creep effect as follows:[7]

$$\Phi = \frac{\varepsilon_{tot} - \varepsilon_{sh} - \varepsilon_{el}}{\varepsilon_{el}} \quad (2), \qquad E_r = \frac{E_1}{1+\Phi} \quad (3)$$

where, ε_{tot}, ε_{sh}, ε_{el} are total strain of a loaded cylinder, free shrinkage of an unloaded cylinder, and elastic strain, respectively, in Eq. 2.

The reduced modulus can be determine using Eq. 3. The Φ values are approximately 0.22 and 0.37 four and 14 days, respectively, after casting the repair material.[6] Incorporating these values, the E_1 is reduced to 82 % and 73 %, respectively, after 4 and 14 days to include the creep effect. It must be noted that the two suggested Φ values were determined only for a specific type of polymer modified cement concrete and, in general, not applicable to any other application: i.e. the Φ values must be experimentally measured.[7]

4. Design procedure

4.1 Shear force estimation

Using the max. τ_{xy} at the interface shown in Tables 3 through 5 and also in Figs. 3 through 5 and the fact that the interface shear stress develops only for the short distance approximately equal to the total thickness ($H_{total} = H_1 + H_2$) of the repaired beam from the end, the shear force acting at the interface can be approximated as the area of a triangle as shown in Fig. 6. The triangular approximation results in the area up to 20 % larger than actual area. Although the differences between the actual and the approximated triangular areas are as much as 20 %, it was decided that the approximation can be used because of the following:

(1) the result is on the conservative side,
(2) the method is easy to apply,
(3) experimentally measured τ_{xy} tends to be larger than analytically determined τ_{xy},[6] probably because the analysis assumes homogeneous material properties and smooth interface and hence does not consider stress concentrations resulting from rough interface.[6]

4.2 Maximum τ_{xy}

The following equations are suggested to be used to determine the maximum τ_{xy} ($\tau_{xy,max}$) developed at the interface:

$$\tau_{xy,max} = C_p C_d \tau_{xy}, \text{ MPa} \quad (4)$$

$$\tau_{xy,max} = C_p C_d \tau^*_{xy}, \text{ MPa} \quad (5)$$

where, in Eq. 4,

C_p = 1.0 for beams and 1 / (1 - ν_1) for slabs;[5] and

C_d = (actual $\Delta\alpha\Delta T$) / (-200 * 10^{-6}) to linearly adjust (increase or decrease) the maximum shear stress following the magnitude of effective strain that is different from -200 * 10^{-6} m/m.

τ_{xy} is determined from Figs. 3 through 5 (or Tables 3 through 5) using the appropriate thickness ratio (m) and the modular ratio (n).

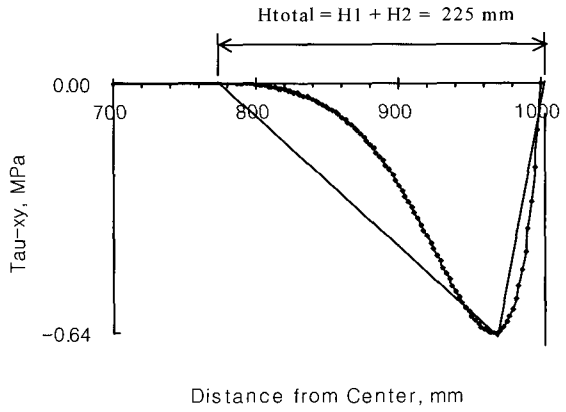

Fig. 6 τ_{xy} Distribution at interface close to end

In Eq. 5, applicable to drying shrinkage-induced stresses, τ_{xy}^* is determined from Figs. 3 through 5 (or Tables 3 through 5) using the thickness ratio (m) and the modular ratio (n) considering the creep effect: i.e. using the reduced modulus, E_r, instead of E_1.

4.3 Required anchor shear strength at interface

The shear force acting at the interface can be determined using Eq. 6.

$$V_{acting} = \tau_{xy,max} * H_{total} / 2 \text{ , N/mm} \quad (6)$$

The shear stress and force determined using Eqs. 4, 5, and 6 represent those developed over a unit width. So, the design shear force (required shear strength) is determined by multiplying the width to V_{acting} obtained from Eq. 6.

$$V_u = V_{acting} * \text{width} \text{ , N} \quad (7)$$

Finally, the design recommendations of references 8-10 can be used to actually design anchors to prevent interface delamination. It is noted that the anchors need to be installed as close as possible to the end to be effective while the distance between center of anchors and concrete edge should be less than H_{total}.

$$V_u \leq \Phi V_n \quad (8)$$

5. Conculsion

An analytical procedure was introduced by which thermally-induced shear stress at interface of repaired concrete beams can be determined. Then a rational method for the anchor design to prevent interface debonding of the repair mortar of the repaired beams or slabs is developed. The design method is also applicable to stresses developed by differential drying shrinkage. So, the proposed anchor design method is inclusive of the effect of temperature change and differential drying shrinkage.

In addition, the results of analytical study that investigated variables influencing the stress development reveal the followings:

1) When a repaired concrete beam or slab is subjected to a temperature change internal stresses develop when the coefficients of thermal expansion of the two materials (repair material and existing concrete) are not the same.
2) The maximum shear stress at the interface is reached very close to the end of the interface.
3) The thickness ratio and the modular ratio of the repair material to those of the existing concrete influence the magnitude of the shear stress.
4) The interface shear stress decreases with decreasing thickness ratio for a constant modular ratio. The interface shear stress also decreases with the decreasing modular ratio for a constant thickness ratio.
5) It is recommended that the thickness and the elastic modulus of the repair material be lowered or use anchors designed following the procedure outlined in this study to prevent debonding at the interface of the repaired concrete members.

Appendix: design example

• **Problem:**

Determine max. τ_{xy} at interface and shear force acting at interface developed in a repaired beam by an ambient temperature drop of 15 °C.

Thickness: H_1 = 30 mm for repair material

H_2 = 300 mm for existing concrete

Elastic modulus: E_1 = 30,000 MPa, E_2 = 25,000 MPa

Thermal coefficient: $\alpha_1 = 15*10^{-6}$ m/m/°C

$\alpha_2 = 10*10^{-6}$ m/m/°C

Ambient temperature change: ΔT = -15 °C

Solution:

Modular ratio, $n = E_1 / E_2 = 30{,}000 / 25{,}000 = 1.2$

Thickness ratio, $m = H_1 / H_2 = 30 / 300 = 0.10$

$\Delta\alpha\Delta T = (15-10)*10^{-6}*(-15) = -75*10^{-6}$ m/m

From Fig. 4 or Table 4 using m = 0.1 and n = 1.2,

$\tau_{xy,} = 0.8386$ MPa

Modification factor for beam, $C_p = 1.0$

Modification factor for actual $\Delta\alpha\Delta T$, $C_d = (-75)/(-200) = 0.375$

Max. shear stress expected to develop in the repaired beam at the interface

$\tau_{xy,max} = 0.375*0.8386 = 0.315$MPa

$V_{acting} = \tau_{xy,max} * H_{total} / 2 = 0.315*330/2 = 52.0$N for 1-mm width

$V_u = 52.0*300 = 15.6$kN

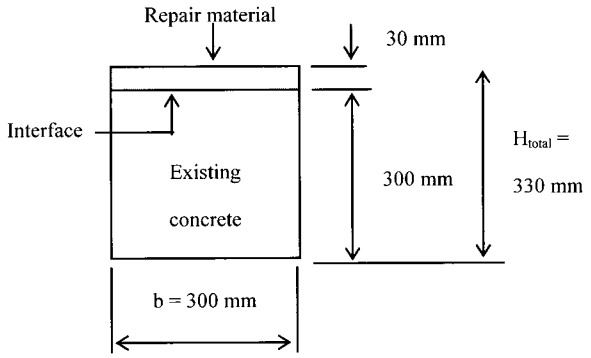

Fig. A Cross-section of a repaired beam

for the total beam width of 300 mm.

Required shear strength that needs to be provided by anchors at the interface by reference 8

$V_n \geq V_u / \Phi = 15.6 / 0.75 = 20.8\text{kN}$

References

1. Won, M. C., Kim S. M.; Merritt D. and McCullough B. F., "Horizontal Cracking and Pavement Distress in Portland Cement Concrete Pavement", the 27th International Air Transport Conference, ASCE, Orlando, Florida, U.S., 2002.
2. Chen, D., Cheng, S., and Gerhardt, T.D., "Thermal Stresses in Laminated Beams", *Journal of Thermal Stresses*, Vol.5, No.1, U.S., 1982, pp.67-84.
3. Hess, M.S., "The End Problem for a Laminated Elastic Strip: Differential Expansion Stress", *Journal of Composite Materials*, Vol.3, U.S., 1969, pp.630-641.
4. Choi, D. U., Fowler, D.W., and Wheat, D. L., "Thermal Stresses in Polymer Concrete Overlays", American Concrete Institute, ACI Special Publication SP-166, *Properties and Uses of Polymers in Concrete*, U.S., 1996, pp.93-122.
5. Fowler, D. W., Choi, D. U., Zalatimo, J., and Wheat, D. L., "Stresses in PC Overlays due to Thermal Changes", ICPIC, *10th International Congress on Polymers in Concrete*, Hawaii, U.S., 2001, in CD-rom.
6. Choi, D. U. and Lee, C. H., "Shrinkage-Induced Stresses at Early-Ages in Composite Concrete Beams", *KCI Concrete Journal*, Vol.14, No.1, Korea, 2002, pp.15-22.
7. Silfwerbrand J., "Stresses and Strains in Composite Concrete Beams Subjected to Differential Shrinkage", *ACI Structural J.*, Vol.94, No.4, 1997, pp.227~238.
8. ACI 318, *Building Code Requirements for Structural Concrete (ACI 318-02) and Commentary (ACI 318R-02)*, American Concrete Institute, U.S., 2002.
9. Fuchs, W., Eligehausen, R., Breen, J.E., "Concrete Capacity Design (CCD) Approach for Fastening to Concrete", *ACI Structural J.*, Vol.92, No.1, 1995, pp.73~94.
10. ACI 349, *Code Requirements for Nuclear Safety Related Concrete Structures (ACI 318-97)*, American Concrete Institute, U.S., 1997.